Journal of Quantitative Spectroscopy & Radiative Transfer 189 (2017) 339–343

Contents lists available at ScienceDirect

Journal of Quantitative Spectroscopy & Radiative Transfer

journal homepage: www.elsevier.com/locate/jqsrt

# Rayleigh scattering and the internal coupling parameter for arbitrary particle shapes

Justin B. Maughan, Amitabha Chakrabarti, Christopher M. Sorensen *

*Department of Physics, Kansas State University, Manhattan, KS 66506, USA*

ARTICLE INFO

*Article history:*
Received 29 September 2016
Received in revised form
2 December 2016
Accepted 5 December 2016
Available online 9 December 2016

*Keywords:*
Light scattering
Rayleigh differential cross section
Q-space
Internal coupling parameter

ABSTRACT

A general method for calculating the Rayleigh scattering by a particle of arbitrary shape is introduced. Although analytical solutions for Rayleigh scattering exist for spheres and ellipsoids, analytical solutions for more complicated shapes don't exist. We find that in general the Rayleigh differential cross section goes as $k^4V^2|\alpha(m)|^2$ where k $= 2\pi/\lambda$ and $\lambda$ is the wavelength, V is the volume of the particle and $\alpha(m)$ the average volume polarizability which is dependent on the shape and the complex index of refraction, m. We use existing computational techniques, the discrete dipole approximation (DDA) and the T-matrix method, to calculate the differential scattering cross section divided by $k^4$ and plot it vs $V^2$ to determine $|\alpha(m)|^2$. Furthermore, we show that this leads to a general description of the internal coupling parameter $\rho'_{arbitrary}=2\pi k\frac{V}{A}|\alpha(m)|$ where A is the average projected area of the particle in the direction of incident light. It is shown that this general method makes significant changes in the analysis of scattering by particles of any size and shape.



## 1. Introduction

The light scattering by regularly and irregularly shaped particles has been the subject of a great deal of theoretical, computational, and experimental work. This work not only advances our knowledge in general, but also plays an important role in climate models. The advancements of computers and computational techniques over the last three decades have made the calculation of light scattering quantities from non-spherical particles more practical as well and greatly increased the speed at which the calculations from spherical particles (Mie scattering) can be calculated. The most common way of presenting the angular patterns of the light scattered intensity from particles is to plot them vs the scattering angle $\theta$, but these are generally not amenable to quantitative description or differentiation for different shapes. Over the past years, we have developed a unique approach that provides quantitative descriptions of angular light scattering patterns produced by particles, Q-space analysis (see Section 2).

The Rayleigh differential cross section for a sphere has a well-known analytical solution which can be found in numerous locations, [1–4] are but a few. An analytical solution for the Rayleigh differential cross section of ellipsoids can also be found in [2,4]. As the shape of the particle begins to become more complicated, finding an analytical solution becomes nearly if not completely impossible. The focus of this work is to present a general description for the Rayleigh scattering cross section of an arbitrary shape and a straightforward method by which it can be calculated using existing computational techniques. It will also be shown that the general definition of the Rayleigh scattering cross section leads to a general definition of the internal coupling parameter [5] as well. Both of these generalizations are important in the application of Q-space analysis to obtain a general description of light scattering by particles of any shape.

## 2. Q-space and the internal coupling parameter for spheres

Our need for a general formulation for the Rayleigh cross section arouse with our application of Q-space analysis to particles of arbitrary shape. Q-space analysis involves plotting the differential scattering cross section (or the scattered intensity) versus q or the dimensionless variable $qR_{eq}$, where $R_{eq}$ is an equivalent radius such as the radius of a sphere $R$, the radius of gyration $R_g$ , or a volume equivalent radius $R_{veq}$, and $q$ is the magnitude of the scattering wave vector: $q = (4\pi/\lambda)\sin\left(\frac{\theta}{2}\right)$ with $\lambda$ being the wavelength and θ is the scattering angle, on a log-log plot [6–8]. Q-space analysis reveals functionalities of the scattering with q that are not apparent with conventional plotting with the scattering angle θ. Often in Q-space analysis, the differential cross section is

* Corresponding author.
*E-mail address:* sor@phys.ksu.edu (C.M. Sorensen).

http://dx.doi.org/10.1016/j.jqsrt.2016.12.004
0022-4073/

normalized by the Rayleigh differential cross section of the particle [8,9] which for a sphere is given by

$$dC_{sca,\ Ray,\ sphere}/d\Omega = k^4R^6\left|\frac{m^2-1}{m^2-1}\right|^2. \tag{1}$$

In Eq. (1) k = $2\pi/\lambda$, m is the relative index of refraction, and the term in the bars is the Lorentz-Lorenz factor. When Q-space analysis is applied to non-spherical particles, a method to determine the proper Rayleigh normalization is needed which is why this work is not only of general intellectual importance but will also play a key role in future Q-space studies.

When the Rayleigh normalized differential cross section of an arbitrary sphere is plotted vs qR, distinct regimes and limits in the scattering curves can be found that would not be apparent when plotting against the scattering angle $\theta$. These regimes appear in the scattering as a function of a parameter that we have named the internal coupling parameter, ρ' [5] that provides a quasi-universal description of the scattering. The internal coupling parameter is derived by looking at the two limits of Mie scattering from spheres. In the $m \to 1$ limit, the Mie scattering from spheres gives the 3d Fraunhofer diffraction limit or the Rayleigh-Debye-Gans (RDG) limit [10]. Looking at the combined $m \to Large$ or $R \to Large$ limit, the scattering is in the 2d Fraunhofer circular aperture (or obstruction) diffraction limit. To define a parameter that describes both of these diffraction limits, we take the square root of the ratio of the differential cross section at zero scattering angle in each limit. For the RDG limit Eq. (1) is used, and for the 2d circular aperture limit the differential cross section is given by [11]

$$\frac{dC_{sca,circle}}{d\Omega}(0) = \frac{k^2R^4}{4}. \tag{2}$$

The square root of the ratio of Eqs. (1) and (2) results in the internal coupling parameter of a sphere given by

$$\rho'_{sphere} = 2kR\left|\frac{m^2-1}{m^2-1}\right|. \tag{3}$$

The internal coupling parameter of a sphere $\rho'_{sphere}$ is related to the Lorentz-Lorenz factor, which is directly involved in the radiative coupling between the sub-volumes that comprise the particle [5]. When $\rho'_{sphere} < 1$, the coupling between sub-volumes is weak, i.e. the effects of internal multiple scattering are small, and thus the scattering is in the RDG limit which corresponds to diffraction from the volume of the particle. As $\rho'_{sphere}$ increases, so does the coupling. As $\rho'_{sphere}$ continues to increase, the scattering approaches the 2d diffraction limit [12].

One of the functionalities that has previously been found in the scattering from spheres is that as $\rho'_{sphere}$ increases past unity, the Rayleigh normalized scattering in the forward direction begins to fall by a factor of $1/\left(\rho'_{sphere}\right)^2$ as shown in Fig. 1. Also, shown in Fig. 1 (right side) is the Rayleigh normalized differential cross section in the forward direction multiplied by $\left(\rho'_{sphere}\right)^2$ which approaches 1 as $\rho'_{sphere}$ goes to infinity.

## 3. Rayleigh scattering for arbitrary shapes

As stated above, descriptions of the Rayleigh differential cross section for spheres can be found in numerous locations [1–4]. It should not be surprising that the Rayleigh differential cross section for a sphere is just a special case of the Rayleigh differential cross section of ellipsoids[2,4]. For randomly oriented ellipsoids the Rayleigh differential cross section is given by [2,4]

$$\frac{dC_{sca,\ Ray,\ ellipsoids}}{d\Omega} = \frac{k^4a^2b^2c^2}{3}\left[\left|\frac{\left(m^2-1\right)}{\left(3+3L_1\left(m^2-1\right)\right)}\right|^2 + \left|\frac{\left(m^2-1\right)}{\left(3+3L_2\left(m^2-1\right)\right)}\right|^2 + \left|\frac{\left(m^2-1\right)}{\left(3+3L_3\left(m^2-1\right)\right)}\right|^2\right] \tag{4}$$

where a, b, and c are the semi-principle axes, and $L_1$, $L_2$,*and* $L_3$ are geometric parameters given by the integrals

$$L_x = \frac{abc}{2}\int_0^\infty \frac{dq}{\left(q+x^2\right)\sqrt{\left(q+a^2\right)\left(q+b^2\right)\left(q+c^2\right)}} \tag{5}$$

with x being equal to a, b, or c for $L_1$, $L_2$,*and* $L_3$, respectively. There are no known analytical results for more complex shapes and finding analytical solutions for Rayleigh scattering by such shapes appears to be extremely difficult, if not impossible. So how can we find the Rayleigh differential cross section for an arbitrary shape?

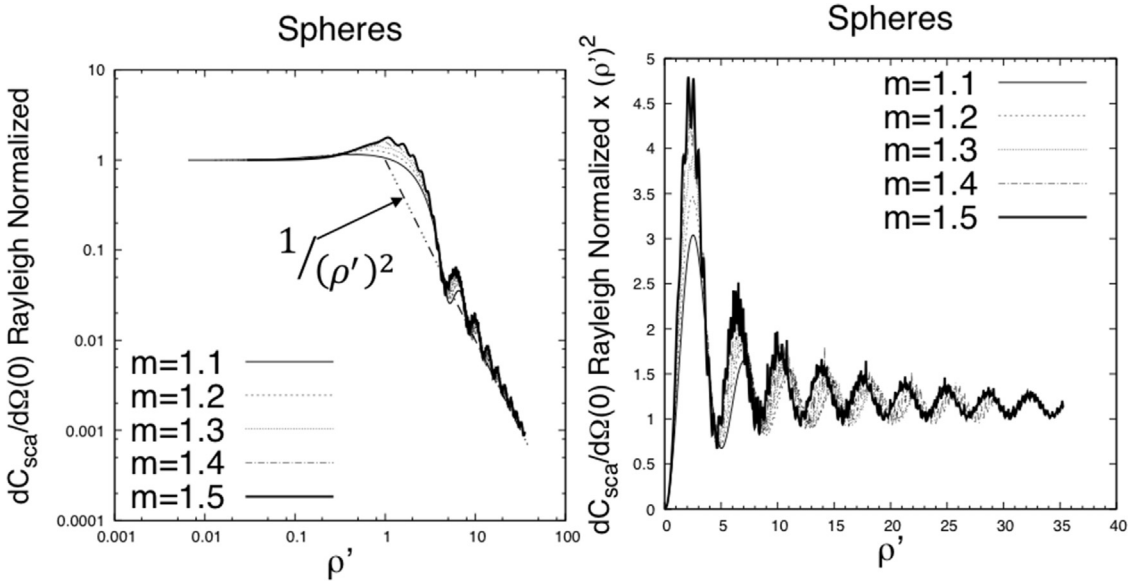


**Fig. 1.** Left: Forward scattered (θ and q = 0) Rayleigh normalized differential cross section of spheres vs $\rho'_{sphere}$. Right: Rayleigh normalized differential cross section x $\left(\rho'_{sphere}\right)^2$ of spheres vs $\rho'_{sphere}$.

van de Hulst [4] gives that in general the Rayleigh differential cross section goes as

$$\frac{dC_{sca,\ Ray,\ arbitrary}}{d\Omega}=k^4V^2\left|\alpha(m)\right|^2 \tag{6}$$

where V is the volume of the particle and $\alpha(m)$ is the average volume polarizability, which is a function of m with functionality dependent on the shape. This can be seen to hold for ellipsoids and spheres by rearranging Eq. (4) in terms of $V=(4/3)\pi abc$ which leads to

$$\left|\alpha(m)\right|^2_{ellipsoids}=\frac{3}{(4\pi)^2}\left[\left|\frac{(m^2-1)}{(3+3L_1(m^2-1))}\right|^2+\left|\frac{(m^2-1)}{(3+3L_2(m^2-1))}\right|^2+\left|\frac{(m^2-1)}{(3+3L_3(m^2-1))}\right|^2\right] \tag{7}$$

For spheroids with $a\neq b=c$, $L_1$=$L_3$ leads to

$$\left|\alpha(m)\right|^2_{spheroids}=\frac{3}{(4\pi)^2}\left[2\left|\frac{(m^2-1)}{(3+3L_1(m^2-1))}\right|^2+\left|\frac{(m^2-1)}{(3+3L_2(m^2-1))}\right|^2\right]. \tag{8}$$

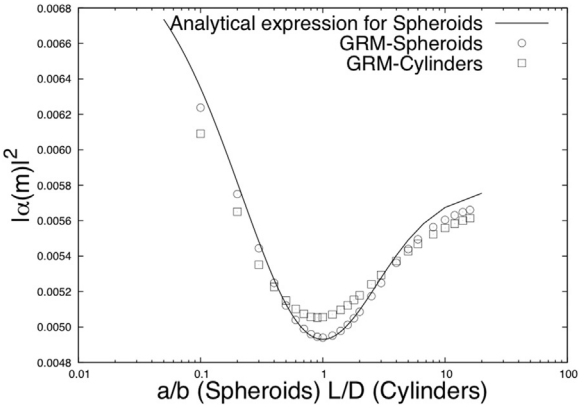


**Fig. 2.** Average volume polarizability square vs a/b for spheroids (open circles) or L/D for cylinders (open squares) both of index m = 1.5. Solid line shows the analytical solution for spheroids calculated with Mathematica.

In the special case of spheres, $L_1$=$L_2$ =$L_3$=1/3 leads to

$$\left|\alpha(m)\right|^2_{spheres}=\frac{9}{(4\pi)^2}\left|\frac{(m^2-1)}{(m^2+2)}\right|^2. \tag{9}$$

Substitutions of Eq. (9) into Eq. (6) yields the well-known equation for the Rayleigh differential cross section for a sphere, Eq. (1).

To find the average volume polarizability $|\alpha(m)|^2$ for a particle of arbitrary shape we will assume that the particle volume and optical wave vector k are known quantities. Using existing computation techniques, such as the discrete dipole approximation (DDA), the differential cross section can be calculated for a series of known volumes within the Rayleigh limit $\lambda \gg$ than the largest linear distance of the particle. All of the optical properties of the particle, such as the complex relative index of refraction, wavelength, volume and shape are handled entirely by the DDA calculations. The differential cross section in the forward direction i.e. ($\theta=0$) divided by $k^4$ can then be plotted vs $V^2$, the slope of which gives $|\alpha(m)|^2$ and thus $|\alpha(m)|$. Once $|\alpha(m)|^2$ is known, the Rayleigh scattering cross section can be calculated for any volume and wavelength for the same particle shape. This procedure, which we call the General Rayleigh Method (GRM), can be used to calculate the Rayleigh scattering cross section for any arbitrary shape.

## 4. Internal coupling parameter for arbitrary shapes

As with spheres, the internal coupling parameter for an arbitrary shape is derived by looking at the $m\rightarrow 1$, 3d diffraction limit and the $m\rightarrow$ *Large* or $V\rightarrow$ *Large*2d diffraction limit. We know from Section 3 that the Rayleigh differential cross section is defined by Eq. (6) and by way of the GRM, the average volume polarizability $|\alpha(m)|^2$ can be calculated. Forward scattering, Fraunhofer diffraction from a two-dimensional arbitrary obstruction is given by [2,4,14,15]

$$\frac{dC_{sca,arbitrary}}{d\Omega}(0)=\frac{k^2A^2}{4\pi^2} \tag{10}$$

where A is the projected area of the three-dimensional shape in the direction of the incident beam. Again, taking the square root of

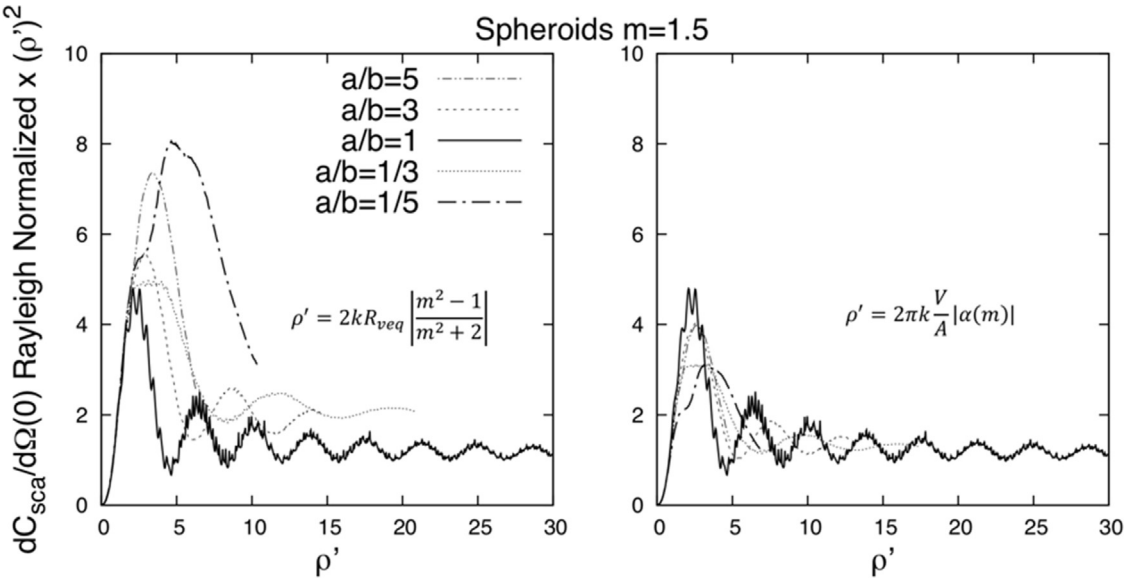


**Fig. 3.** Left: Rayleigh normalized differential cross section of spheroids x $\left(\rho'_{sphere}\right)^2$ vs $\rho'_{sphere}$ using the volume equivalent radius. Right: Rayleigh normalized differential cross section of spheroids x $\left(\rho'_{arbitrary}\right)^2$ vs $\rho'_{arbitrary}$.

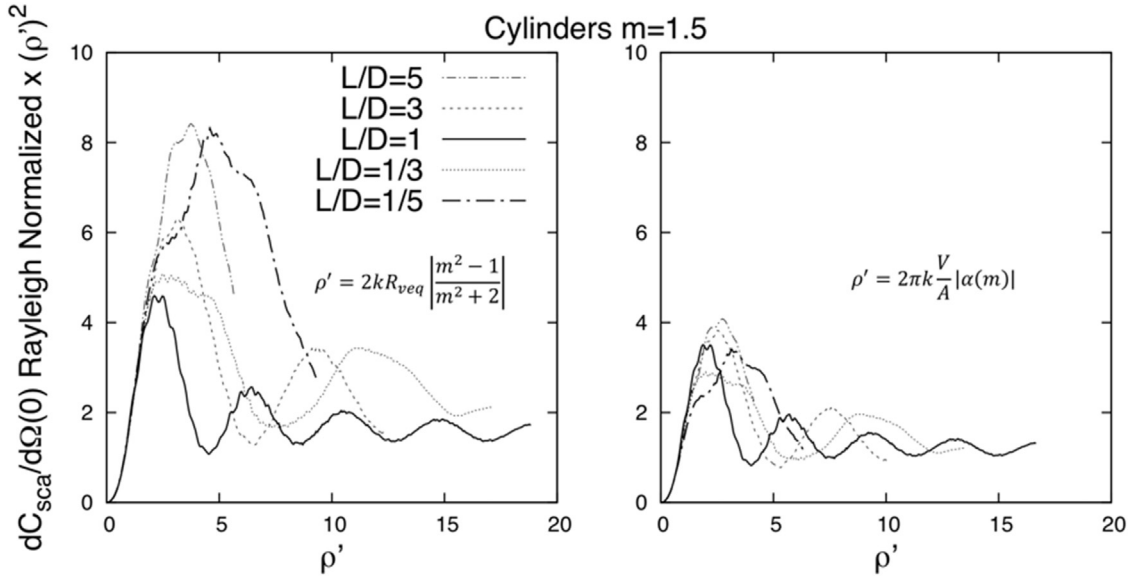


**Fig. 4.** Left: Rayleigh normalized differential cross section of cylinders x $\left(\rho'_{sphere}\right)^2$ vs $\rho'_{sphere}$ using the volume equivalent radius. Right: Rayleigh normalized differential cross section of cylinders x $\left(\rho'_{arbitrary}\right)^2$ vs $\rho'_{arbitrary}$.

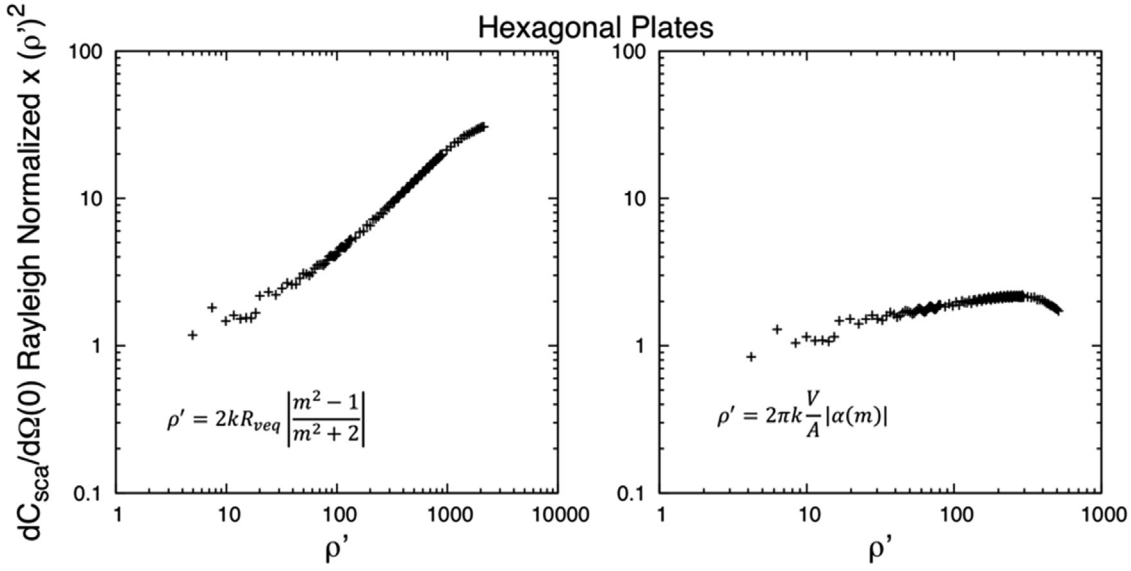


**Fig. 5.** Left: Rayleigh normalized differential cross section of hexagonal plates x $\left(\rho'_{sphere}\right)^2$ vs $\rho'_{sphere}$ using the volume equivalent radius. Right: Rayleigh normalized differential cross section of hexagonal plates x $\left(\rho'_{arbitrary}\right)^2$ vs $\rho'_{arbitrary}$. The index of refraction is m = 1.31.

the ratio of these two limits results in

$$\rho'_{arbitrary}=2\pi k\frac{V}{A}|\alpha(m)| \tag{11}$$

Eq. (11) is a general definition for the internal coupling parameter for any arbitrary shape, of which Eq. (3) is a specific case for spheres.

## 5. Results

Fig. 2 shows a comparison of $|\alpha(m)|^2$ for spheroids with m = 1.5 calculated using the General Rayleigh Method (GRM) described above, and the analytical solution of Eq. (2) calculated using Mathematica [16] for a range of axial ratio $a/b$. When axial ratio $a/b > 1$ the spheroid is prolate (cigar) and if $a/b < 1$ it is oblate (disk), and when equal to unity a sphere. To calculate the shape and index dependent $|\alpha(m)|^2$ using the GRM, ADDA [17], a well-known and widely used software for calculating the scattering by arbitrary shapes, was used. It can be seen in Fig. 2 that the GRM agrees well with the analytical solution, only deviating slightly as the axial ratio $a/b$becomes extreme. This is more likely due to errors in calculations of the differential cross section by ADDA and not the GRM. Fig. 2 also shows the results of the application of the GRM to cylinders with m = 1.5; here the shape dependence of $|\alpha(m)|^2$ can be seen. When the ratio $L/D = 1$ where D is the diameter and L is the length of the cylinder, the $|\alpha(m)|^2$ term for cylinders sits slightly above the spheroids, but still follows the general trends of spheroids as the shape is elongated or flattened.

To investigate the validity of $\rho'_{arbitrary}$ and the GRM, a freely available and widely used T-Matrix (TM) code developed by Mishchenko and Travis [18] was used to calculate the differential scattering cross section for both spheroids and cylinders. The

differential cross sections were calculated for axial ratios or length to diameter ratios of spheroids and cylinders, respectively of $\frac{a}{b}$ or $\frac{L}{D}$=1/5, 1/3,1,3,5 at indexes $m$ = 1.1,1.2,1.3,1.4,1.5, for a range of volume equivalent size parameters approaching the limit of capabilities of the TM code, see [18]. Figs. 3 and 4 show a comparison of the differential cross section in the forward direction (i.e. $\theta = 0$), normalized by the Rayleigh differential cross section and multiplied by $(\rho')^2$ versus $\rho'$ for spheroids and cylinders, respectively. The GRM and $\rho'_{arbitrary}$ are used on the (right) and using the Rayleigh differential cross section of a sphere and $\rho'_{sphere}$ (left) for a range of axial ratios $a/b$ for spheroids, or length to diameter ratios $L/D$ for cylinders. It is important to remember that if the Rayleigh normalized differential cross section truly goes as $1/\left(\rho'_{arbitrary}\right)^2$ then as $\rho'_{arbitrary}\rightarrow\infty$ the curves in Figs. 3 and 4 should go to $\sim$1. When using the definitions specific to spheres, as the axial ratios move away from unity, the first initial peak is as much as two times that of spheres. In the case of spheroids or compact cylinders, the curves also appear to be approaching an asymptote of increasingly higher values as aspect ratio moves away from unity and not all going to $\sim$1 as $\rho'_{sphere}\rightarrow\infty$. Whereas when the GRM and $\rho'_{arbitrary}$ is used, all of the ratios remain within the same envelope and appear to be approaching $\sim$1 as $\rho'_{arbitrary}\rightarrow\infty$. Simply said: for non-spherical shapes the forward scattering is better described by using the generalized expressions for the Rayleigh scattering and the internal coupling parameter.

The improvements demonstrated in Figs. 3 and 4 are small but important as the Q-space analysis of non-spherical shapes continues. Recently Q-space analysis has been applied to ice crystals [13], in which the GRM and $\rho'_{arbitrary}$ leading to improvement of about an order of magnitude for some of the ice crystal shapes considered. For example, Fig. 5 shows a similar comparison as shown in Figs. 3 and 4 for hexagonal plates; the data presented is from a database of the single-scattering properties reported by Yang et al. [19]. As can be seen on the left of Fig. 5, when the sphere Rayleigh differential cross section and $\rho'_{sphere}$ are used to study the forward scattering of these plates, the Rayleigh normalized forward scattering varies over a range of $\sim$30. On the other hand, Fig. 5 shows on the right when the GRM is used for Rayleigh normalization and $\rho'_{arbitrary}$, the data is more tightly grouped over a range of $\sim$2 as $\rho'_{arbitrary}$ increases.

## 6. Conclusions

The General Rayleigh Method (GRM) has been shown to be a straightforward method for calculating the average volume polarizability, and thus the Rayleigh scattering for an arbitrary shape. It has also been shown that the general definition of Rayleigh scattering for arbitrary shapes leads to the general definition of the internal coupling parameter for any shape, of which the spherical definition is a special case. When the GRM and the internal coupling parameter for arbitrary particles is used in connection with Q-space analysis, similar functionalities and behaviors as have been previously found with spheres are found in the scattering patterns of cylinders, ellipsoids, hexagonal plates, ice crystals [13] and, we anticipate, many other shapes. This work provides a firm basis for the future application of Q-space analysis of the light scattering from irregular particles.

## References


[1] J.D. Jackson. Classical electrodynamics. USA: Massachusetts; 1998.
[2] Bohren CF, Huffman DR. Absorption and scattering of light by small particles. New York: Wiley; 1983.
[3] Kerker M. The Scattering of light and other electromagnetic radiation. New York: Academic Press; 1969.
[4] van de Hulst HC. Light scattering by small particles. New York: Wiley; 1957.
[5] Heinson WR, Chakrabarti A, Sorensen CM. A new parameter to describe light scattering by an arbitrary sphere. Opt Commun 2015;356:612–615. http://dx.doi.org/10.1016/j.optcom.2015.08.067.
[6] Sorensen CM, Fischbach DJ. Patterns in Mie scattering. Opt Commun 2000;173:145–153. http://dx.doi.org/10.1016/S0030-4018(99)00624-0.
[7] Sorensen CM, Shi D. Patterns in the ripple structure of Mie scattering. J Opt Soc Am -Opt Image Sci Vis 2002;19:122–125. http://dx.doi.org/10.1364/JOSAA.19.000122.
[8] Sorensen CM. Q-space analysis of scattering by particles: a review. J Quant Spectrosc Radiat Transf 2013;131:3–12. http://dx.doi.org/10.1016/j.jqsrt.2012.12.029.
[9] Berg MJ, Sorensen CM, Chakrabarti A. Patterns in Mie scattering: evolution when normalized by the Rayleigh cross section. Appl Opt 2005;44:7487–7493. http://dx.doi.org/10.1364/AO.44.007487.
[10] Sorensen CM. Q-space analysis of scattering by particles: a review. J Quant Spectrosc Radiat Transf 2013;131:3–12. http://dx.doi.org/10.1016/j.jqsrt.2012.12.029.
[11] Hecht E. Optics. Addison-Wesley; 2002.
[12] Heinson WR, Chakrabarti A, Sorensen CM. Crossover from spherical particle Mie scattering to circular aperture diffraction. J Opt Soc Am -Opt Image Sci Vis 2014;31:2362–2364. http://dx.doi.org/10.1364/JOSAA.31.002362.
[13] Heinson YW, Maughan JB, Ding J, Chakrabarti A, Yang P, Sorensen CM. Q-space analysis of light scattering by ice crystals. J Quant Spectrosc Radiat Transf 2016;185:86–94. http://dx.doi.org/10.1016/j.jqsrt.2016.08.021.
[14] Bohren CF, Koh G. Forward-scattering corrected extinction by nonspherical particles. Appl Opt 1985;24:1023. http://dx.doi.org/10.1364/AO.24.001023.
[15] Born M, Wolf E, Bhatia AB. Principles of Optics: Electromagnetic Theory of Propagation, Interference and Diffraction of Light. Cambridge: Cambridge University Press; 1999.
[16] Mathematica. n.d.
[17] Yurkin MA, Hoekstra AG. The discrete-dipole-approximation code ADDA: capabilities and known limitations. J Quant Spectrosc Radiat Transf 2011;112:2234–2247. http://dx.doi.org/10.1016/j.jqsrt.2011.01.031.
[18] Mishchenko MI, Travis LD. Capabilities and limitations of a current FORTRAN implementation of the T-matrix method for randomly oriented, rotationally symmetric scatterers. J Quant Spectrosc Radiat Transf 1998;60:309–324. http://dx.doi.org/10.1016/S0022-4073(98)00008-9.
[19] Yang P, Bi L, Baum BA, Liou K-N, Kattawar GW, Mishchenko MI, et al. Spectrally Consistent Scattering, Absorption, and Polarization Properties of Atmospheric Ice Crystals at Wavelengths from 0.2 to 100 mu m. J Atmos Sci 2013;70:330–347. http://dx.doi.org/10.1175/JAS-D-12-039.1.